Breaking the Capacity-Polarization Trade-off in Li-O_2 Batteries through Dual-Modulation of Hierarchical Porosity and Active Site Configurations in ZIF-Derived Electrocatalysts

Xinrong Hu[1], Meiling Wang[3], Feiyang yang[1], Zhaolin Gou[1], Ziyi Chen[1], Qike Xu[1], Cunzhong Zhang[1], Yuefeng Su[1,2], Ying Yao[1,2*]

[1] Beijing Key Laboratory of Environmental Science and Engineering, School of Materials Science & Engineering, Beijing Institute of Technology, Beijing 100081, China

[2] Zhengzhou Research Institute, Beijing Institute of Technology, Zhengzhou 450000, China

[3] Institute of Systems Science, Beijing Wuzi University, Beijing 101149, China

* Corresponding author, E-mail: yaoying@bit.edu.cn

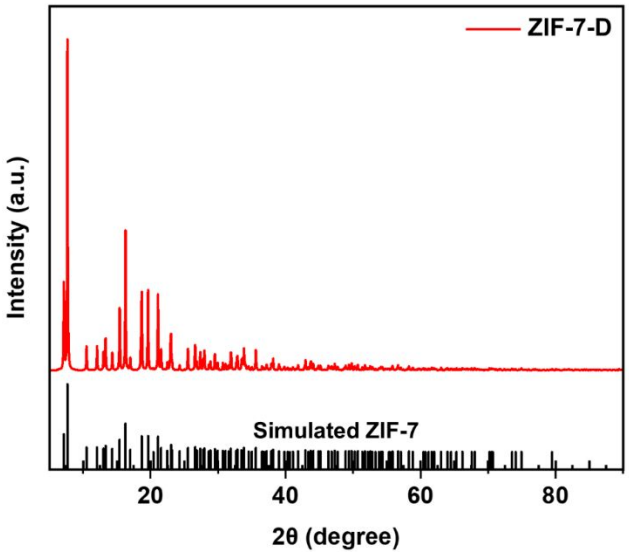

Fig S1. XRD of XRD pattern of precursor ZIF-7 crystals.

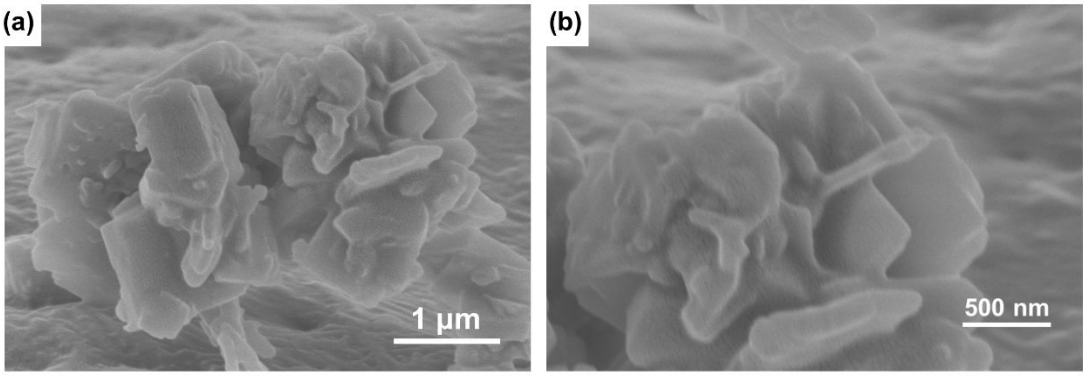

Fig S2. SEM images of ZDC in different magnifications.

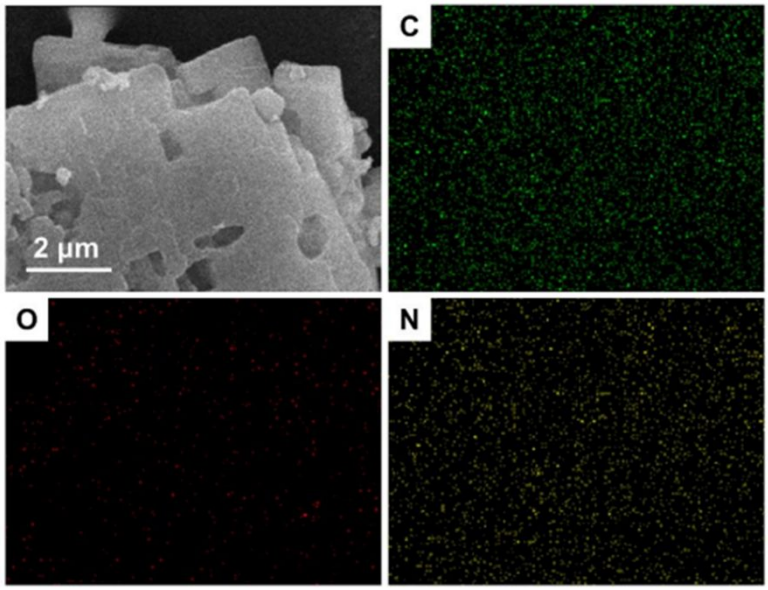

Fig S3. SEM images and corresponding element mapping images of ZDC.

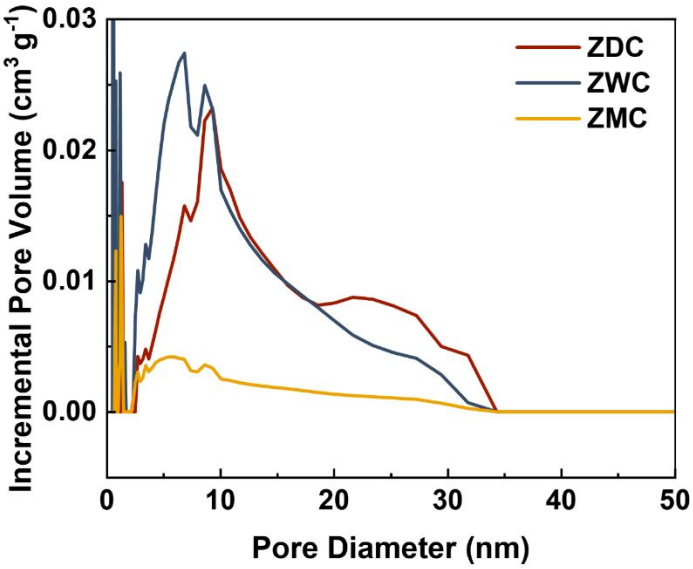

Fig S4. NLDFT micropore analysis of ZDC, ZWC and ZMC.

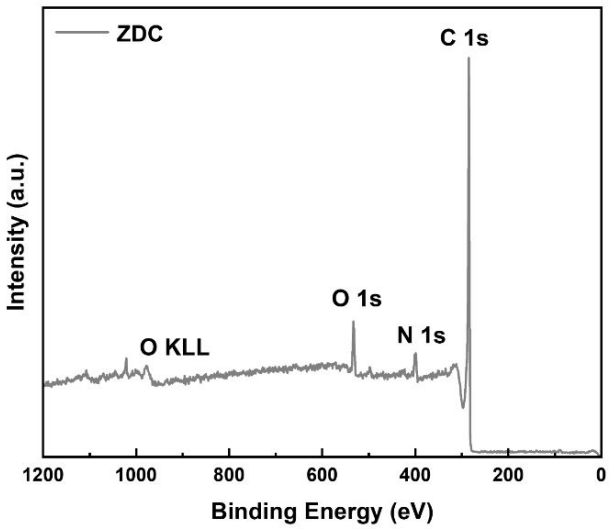

Fig S5. XPS survey spectrum of ZDC.

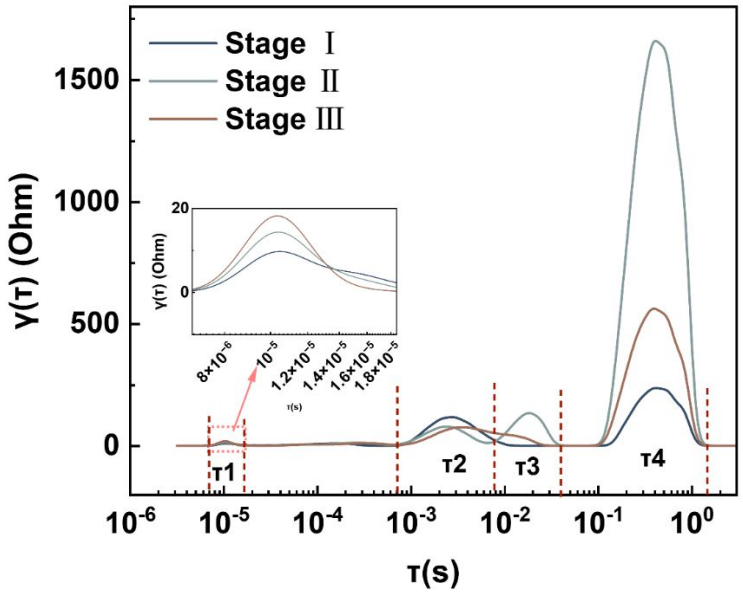

Fig S6. DRT plots obtained by deconvolving the EIS at different stages of discharge and charge.

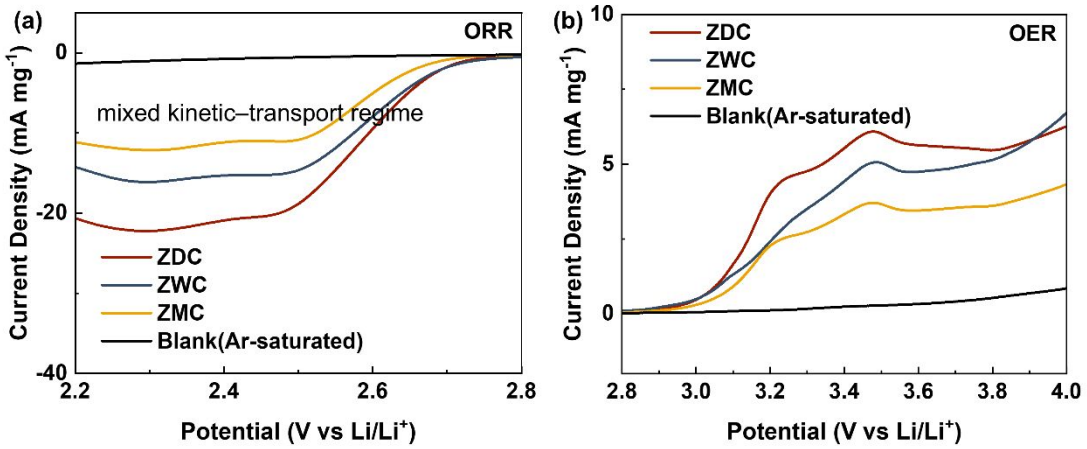

Fig S7. LSV curves of ZDC, ZWC and ZMC in O2 saturated 1 M LiTFSI/TEGDME solution and ZDC in Ar-saturated 1 M LiTFSI/TEGDME solution.

Table S1 The BET specific surface areas, average pore size and pore volume of ZDC, ZWC and ZMC.

Sample	S_{BET} (m^2 g^{-1})	Average pore Size (nm)	Pore volume (cm^3 g^{-1})
ZDC	554.37	6.4	0.55
ZWC	933.67	5.4	0.81
ZMC	253.26	5.5	0.18

Table S2 Element atomic contents in ZDC, ZWC and ZMC.

Sample	Atomic content (at%)		
	C	N	O
ZDC	88.53	5.53	5.93
ZWC	87.56	6.52	5.92
ZMC	81.38	5.74	12.88

Table S3 N moiety contents in ZDC, ZWC and ZMC.

Sample	Relative content of N species (at%)			
	Pyrrolic-N	Pyridinic-N	Graphitic-N	Oxidized-N
ZDC	12.98	34.97	44.15	7.90
ZWC	48.54	11.73	30.34	9.39
ZMC	20.66	33.66	25.63	20.66

Table S4 Comparison of the discharge specific capacity and cycle time of carbon-based Li-O_2 batteries reported in the literature.

Samples	Current density (mA g^{-1})	Discharge specific capacity (mAh g^{-1})	Cycling time (h)/Limited capacity (mAh g^{-1})	Charge overpotential (V)	References
Cobalt Oxides	100	13331	1400/1000	1.15 V	[1]
Co_3O_4/CeO_2 p-n Heterojunction in-situ Embedded in Co/N-Carbon Nanofiber	100	9667.3	700/500	1.96 V	[2]
Activated Co/N Doped Carbon Nanotube/Carbon Nanofiber Composites	100	11512.4	1300/500	0.76V	[3]
Amorphous/crystalline Heterostructure CoFeCe Oxide	100	12340	2900/1000	1.7 V	[4]
Atomic Fe-dispersed Hollow Carbon Nanocage Supporting Ru-Pd Binary Nanoclusters	100	31211	6000/1000	1.98 V	[5]
Ru nanoparticles mounted on FeCo/N-rGO	200	23905/200	1800/600	0.9 V	[6]
Biomass-derived 3D Hierarchical N-doped Porous Carbon Anchoring Co-Fe Phosphide Nanodots	100	11969	2820/1000	1.35 V	[7]
Metal-free N-doped porous carbon	100	21395	2500/500	0.77V	This Work

[1] Liu XM, Zhao LL, Xu HR, Huang QS, Wang YQ, et al. 2020. Tunable Cationic Vacancies of Cobalt Oxides for Efficient Electrocatalysis in Li-O₂Batteries. *ADVANCED ENERGY MATERIALS* 10https://doi.org/10.1002/aenm.202001415

[2] Guo S, Wang J, Sun Y, Peng L, Li C. 2023. Interface engineering of Co3O4/CeO2 heterostructure in-situ embedded in Co/N-doped carbon nanofibers integrating oxygen vacancies as effective oxygen cathode catalyst for Li-O2 battery. *Chemical Engineering Journal* 452:139317. https://doi.org/https://doi.org/10.1016/j.cej.2022.139317

[3] Yang Z-D, Yang X-Y, Liu T, Chang Z-W, Yin Y-B, et al. 2018. In Situ CVD Derived Co–N–C Composite as Highly Efficient Cathode for Flexible Li–O2 Batteries. *Small* 14:1800590. https://doi.org/https://doi.org/10.1002/smll.201800590

[4] Sun ZH, Cao XC, Tian M, Zeng K, Jiang YX, et al. 2021. Synergized Multimetal Oxides with Amorphous/Crystalline Heterostructure as Efficient Electrocatalysts for Lithium-Oxygen Batteries. *ADVANCED ENERGY MATERIALS* 11https://doi.org/10.1002/aenm.202100110

[5] Huang LL, Zhang LH, Liu MR, Zhang QH, Chen ZS, et al. 2023. Nitrogen and atomic Fe co-doped hollow carbon nanocages supporting RuPd nanoclusters as extraordinary high-performance nanoreactor-like cathode for lithium-oxygen batteries. *ENERGY STORAGE MATERIALS* 61https://doi.org/10.1016/j.ensm.2023.102874

[6] Zeng XY, You CH, Leng LM, Dang D, Qiao XC, et al. 2015. Ruthenium nanoparticles mounted on multielement co-doped graphene: an ultra-high-efficiency cathode catalyst for Li-O₂ batteries. *Journal of Materials Chemistry A* 3:11224-11231. https://doi.org/10.1039/c5ta01887k

[7] Sun KL, Li J, Huang LL, Ji S, Kannan P, et al. 2019. Biomass-derived 3D hierarchical N-doped porous carbon anchoring cobalt-iron phosphide nanodots as bifunctional electrocatalysts for Li-O₂ batteries. *JOURNAL OF FiPOWER SOURCES* 412:433-441. https://doi.org/10.1016/j.jpowsour.2018.11.079